Optimization of Direct Laser Deposition Process for Shot Sleeves Used in Aluminium Diecasting

Bibin Babu[#] M. Muthukumaran[*]

[#] *PG Research Scholar *Supervisor*

[#,*] *Department of Mechanical Engineering, SNS College of Engineering, Coimbatore, India*

Abstract **- Optimization is a process or a methodology of making something a fully functional, perfect, effective as possible. In product design optimization of the design is the most economical and creating efficient design. By using product models either by hand or through several different software programs optimal product can be done. In this paper a Direct Laser Deposition (DLD) method is applied to create shot sleeve prototype. A laser beam is used to fuse metal powder onto a substrate in the form of many layers and the part is gradually fabricated to near net-shape. The shot sleeves used in aluminium die casting produced by laser deposition method is optimized. Shot sleeves are critical elements for aluminium die casting through which the molten medium is transferred into the die. H13 Tool steel is used as the deposit material and the 316L stainless steel as the substrate material. The micro structural properties like the knoop hardness, dendrite size, secondary dendrite arm spacing (SDAS) ASTM grain size, the build rate and the porosity are used as the evaluation criteria. The experiment is conducted in random order and the analysis are obtained by minitab software.**

Key Words **- Direct Laser Deposition Process, Die casting, Rapid prototyping, Tool Steels, ANOVA**

I. INTRODUCTION

In recent years, additive manufacturing processes, characterized by layer upon layer construction of parts, have emerged as an alternative to conventional processes for the manufacturing of various metal materials like steel, aluminum and titanium alloys.

Direct metal deposition (DMD) is an advanced additive manufacturing technology which is attracting increasing interest due to its suitable applicability in maintenance, repair and overhaul of critical high-cost products, such as those employed in the aerospace and automotive industry. These complex products may be subject to manufacturing-induced damages or to severe operating conditions (temperature, wear, and mechanical stresses) hindering the product's operational functionality in both cases, to avoid scrap part replacement, which create high costs, proper part recovery operations are required.

A. Rapid Prototyping

The recent improvement of RP technologies can be closely linked with the developments computer technologies costs of computer technologies and advancements many computer-related areas including CAD, CAM, and CNC machining tools approaches have completely changed today's factors functions. The existence of RP system would not have been possible unless these computer technologies evolved with reduction in costs. Moreover, many other technologies and advancements in other fields such as Manufacturing systems and materials have also played pivotal roles in the development of RP technologies

B. Direct Laser Deposition

In laser direct metal deposition, a laser beam is used as a focused heat source to scan the surface and create a melting pool over an existing metal substrate. Since the added metal impinging the molten pool is fed simultaneously with the laser action in the form of wire or loose powder, a deposited metal trace is generated with metallurgical bonding to the substrate as a result of fusion and diffusion phenomena.

Laser direct metal deposition allows for minimal distortion of the work piece, reduced heat affected zones, and superior surface quality. Moreover, the coating adherence and its tribological behavior are reported to be higher in laser DMD. Another interesting aspect of DMD technology is the possibility to achieve enhanced productivity, higher process automation, and reduction of the overall process time, which are main targets within adaptive and flexible manufacturing environments typical of the factories of the future .Single weld tracks are placed next to each other in order to form a single layer with thickness varying from 0.1 mm to several millimeters depending on the process parameters. In order to coat wide surfaces on 3D complex geometries, side overlapping of the individual laser traces is required. The process can be utilized in the repair of worn out high value components, the building of new components, and the application of wear resistant and corrosion resistant coatings.

Direct laser deposition (DLD) or direct metal deposition (DMD) process is a laser- assisted direct metal manufacturing process that uses computer controlled lasers that, in hours, weld air blown streams of metallic powders into custom parts and manufacturing moulds. Some processes use wire instead of powder, but the concept is similar. A representative process is called the Laser Engineered Net Shaping (LENS) process. It

uses CAD life cross-sections to control the forming process developed by Optomec Inc. The DLD process can be used throughout the entire product life – cycle for applications ranging from materials research to functional prototyping to volume manufacturing. An additional benefit is its unique ability to add material to existing components for service and repair applications. Powder metal particles are delivered in a gas stream into the focus of a laser to form a molten pool of metal. It is a layer – by – layer additive rapid prototyping process. The DLD process allows the production of parts, moulds, and dies that are made out of the actual end material, such as aluminium or tool steel. In other words, this produces the high – temperature materials that are difficult to make using the traditional RP processes.

C. Problem Statement

This paper addresses a problem about conducting DOE optimization of the laser deposition process using an H13 tool steel as the deposit material and 316L stainless steel as the substrate material. Stainless steel is corrosion resistant, whereas tool steel is known for its inherent toughness.

As the grain size of H13 becomes coarser or larger, the elongation, fatigue strength impact transition temperature, etc. decrease. This is correlated to dislocation cracks that result from the coalescence of dislocations increasing with the grain size. Coarse grained steels are also inferior when it comes to bending and fatigue testing. Moreover, coarse grained materials are more prone to distortion and are more prone to crack during quenching or grinding. In a normalized condition, the coarse grained steel is preferred during machining but when finishing the part like grinding and polishing, a fine grain is preferred. In this process, an equiaxed grain with the least possible grain size is desired as further heat treatment would be necessary to change the microstructure depending on the application.

D. Experimental Procedure

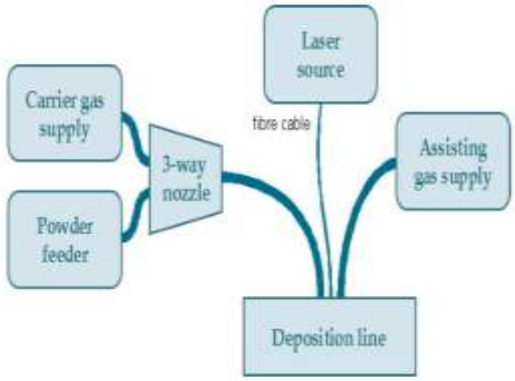

Fig. 1 Main components of laser deposition line

1. Selection Factors And Levels

TABLE I Selection of Factors and Levels

Sl. No	Control Factors	Levels		
		1	2	3
1.	Laser power (P) watt	500	750	1000
2.	Spot size (D) mm	0.71	0.74	0.81
3.	Inner gas pressure (IG) psi	3	4	-
4.	Outer gas pressure (OG) psi	8	10	12
5.	Feedrate (F) ipm	20	25	30
6.	Powder florate (PF) g/min	8	10	12
7.	Percentage overlap (O) %	25	35	45

A total of seven factors were chosen as control factors with 3 levels except for the inner gas pressure, which was set at 2 levels as shown in Table 1. To decide upon the actual values of the levels, a series of experiments were conducted and the range of each factor was determined. A feasible range of a factor would always give a satisfactory deposition that would bond with the substrate and not delaminate. A set of extreme factor combinations (e.g. lowest laser power, highest traverse speed, highest gas pressure, highest powder flow rate, lowest overlap factor, and lowest spot size) were chosen and tested for a satisfactory deposition with good bonding onto the substrate and no de-lamination. If not, the suitable factor range was reduced and the process repeated until a good result was obtained.

2. Orthogonal Array

The number of factors and their levels determine the choice of an OA. For this setup, the L18 OA as shown in Table was chosen with the remaining column allocated for the noise factors and the interactions. By doing this, a good estimate of the contribution of the noise and interactions can be done and the process compensated to behave desirably in their presence, i.e., their effect minimized on the process. The numbers in the error column can be treated as the levels of the error control factors.

3. Sample Preparation

The sample depositions were 0.5” x 0.5” and the deposition was continued until at least a 0.2” height was obtained. Three samples were a made for each experiment to ensure repeat ability. The build rate was calculated for all the samples and they were sectioned using an abrasive water-jet for cross-sectional evaluation as well as evaluation on the top surface. Then they were hot-mounted in Bakelite. The mounts were then ground and polished to 0.5 um surface finish

There are around 248 etching methods that have been used until now. For the samples, preferential etching was conducted. Preferential etching, also known as anisotropic etching is done by using an etchant that attacks different

crystallographic planes at different rates and produces an image controlled by those planes. Initially 2%Nital (2 ml HNO3 +98ml ethanol was used to etch the samples. Later 4% picric acid (96% water as a base) was tried out and the macro structural images were found to be slightly better than with Nital.

TABLE II Orthogonal Array

Exp No.	laser power (Watt)	Spot size (mm)	Feed rate imp	Powder flow rate (g/min)	Overlap factor (%)	Inner Gas pressure (psi)	Outer Gas pressure (psi)	Error
1	500	0.21	20	8	25	4	8	1
2	500	0.25	25	10	35	4	10	2
3	500	0.3	30	12	45	4	12	3
4	750	0.25	20	8	45	4	10	3
5	750	0.3	25	10	25	4	12	1
6	750	0.21	30	12	35	4	8	2
7	1000	0.3	20	10	35	4	8	3
8	1000	0.21	25	12	45	4	10	1
9	1000	0.25	30	8	25	4	12	2
10	500	0.25	20	12	35	5	12	1
11	500	0.3	25	8	45	5	8	2
12	500	0.21	30	10	25	5	10	3
13	750	0.21	20	10	45	5	12	2
14	750	0.25	25	12	25	5	8	3
15	750	0.3	30	8	35	5	10	1
16	1000	0.3	20	12	25	5	10	2
17	1000	0.21	25	8	35	5	12	3
18	1000	0.25	30	10	45	5	8	1

4. Responses

Many response, also known as criteria, were used in this study. They are the build rate in mm^3/s, micro-hardness (Knoop hardness), grain sizes, SDAS, cracks, and porosity. For the build rate, the dimensions of the sample (bild volume) were measured using a Lab view progress that measured the total movement time of the CNC machine axes very accurately. The SDAS reduces with increase in cooling rate of the deposit. The material properties improve when the SDAS gets finer. Long secondary arms would result in inter-dendritic shrinkage or shrinkage porosity. Smaller primary arms would help avoid this condition. Fe3C forming in steel increase the strength of the material. The Knoop hardness was measured on the top surface as well as the cross sections where the hardness was measured at various levels to defect any trend in the process. The cracks were measured from the photomicrograph of the sample at 100 x magnification using image processing. As the cracks were darker than the deposit, the area covered by the cracks could be calculated. The samples were ranked from a scale of 1-5 based on the percentage of cracks (ranging from 0% to around 15%) with 5 being the best and I being the poorest. The ASTM grain size was calculated using the Heyn intercept counting (Dehoff68, Voort84). This method is faster than Other methods because only the grains in the perimeter are counted. The number of grain boundary in intercepts per unit length N_L is given by,

$$N_L = \frac{M\Sigma P_t}{L_t}$$

Where ΣP_1 is the total number of grain boundary intercepts, M is the magnification and L, is the length of the reference line used for counting the intercepts. The ASTM grain size is given by,

$$G = (6.6353 \log NL) - 12.6$$

All these responses were combined into one single entity called the OFC.

5. Formulation The Overall Evaluation Criterion

As discussed before, in order to form the OEC, a certain weigh percentage must be allocated to each QC using the weigh distribution method. Assume that the build rate, hardness, SDAS, grain size, and the cracks or porosity were each given the same weight percentage. The individual sample readings were not listed in the experiment table. There were three readings taken for each QC on each sample. Only their mean values are shown in Table. The OEC is formulated as a larger – the better case for the hardness (H) and build rate (B); and smaller –the-better for the remaining ZCs, such as porosity (P), dendrite (D), etc. From Equations, one can obtain,

$$OEC = \left\{\frac{QC_{H-QC_{\min}(H)}}{QC_{\max(H)-QC_{\min}(H)}} \times W_H\%\right\} + \left\{\frac{QC_{B-QC_{\min}(B)}}{QC_{\max(B)-QC_{\min}(B)}} \times WB\%\right\}$$

$$\left\{\left(1 - \frac{QC_{\max(p)-QC_p}}{QC_{\max(p)-QC_{\min}(p)}} \times W_p\%\right)\right\} + \left\{\left(1 - \frac{QC_{\max(D)-QC_D}}{QC_{\max(D)-QC_{\min}(D)}} \times W_D\%\right)\right\}$$

6. Experimentation

The experiment was conducted in random order. The order was randomly generated by Minitab software and each experiment was repeated three times. The results from the experiment are shown in Table. The weight age of the criteria in the OEC was changed to different combinations and the result studied for the sake of comparison.

7. Analysis of the Mean

The ANOM is used to do a two step optimization by reducing the variation in the process first (using the S/N ratio and maximizing the slope) and then shifting the mean or target performance to get an optimized result or response.

Reducing the variation in a process in often more difficult than shifting the mean. The ANOM was conducted next, as shown in Tables and the factor level plots of the means were constructed as shown. The levels of the control factors with the highest S/N ratio were used in corroboration of the predicted values for the confirmation experiment. The optima levels for an equal OEC are laser power III, federate III, powder flow rate III, inner gas II, outer gas III, spot size II, and overlap factor III

8. Analysis of the Variance

The percentage contributions of the factors are shown in Figure 2. It can be seen that the laser power, overlap factor, and the inner gas contribute 68% of the total process influence. This implies that they have a fair deal of control over this process when compared to the others.

The degree of freedom (or df) of a factor effect is one less than the number of levels for that factor. For this experiment, the total df is 39 for three repetitions of each experiment. The L18 array has an empty column with 3 levels (df =2). This column can be allocated to the interactions and error to study their effects on this process.

The laser power, overlap factor, inner gas, federate, and power flow rate have been chosen as significant control factors and the remaining factors have been pooled together as the error.

TABLE III Analysis of the mean

	Inner gas	Laser	Feed rate	Powder	Outer gas	Spot	Overlap
	Pressure	Power		Flow rate	Pressure	Diameter	Factor
Mean	PSI	Watt	IPM	g/min	PSI	mm	%
1	56.58	40.92	46.34	44.24	49.41	54.12	41.57
2	60.23	49.30	50.06	52.05	49.96	50.53	53.76
3	-	63.08	56.90	57.01	53.22	48.65	57.96

TABLE IV Sum of square

Description	$(dB)^2$
Grand total sum of squares	26789.45
Total sum of squares	161.20
Sum of squares due to the mean	26628.25

TABLE V Design of experiments using L18 Array

									Average Values						Responses			
									Build	Hardness	Porosity	Dendrite	SDAS	Grain				
EXP	IG	P	F	PF	OG	D	O	Err	Rate	Knoop	Rank	size		size	mean	S/N	Mean	S/N
NO	PSI	WATT	IPM	g/mn	PSI	MM	%		mm3/s	HK				ASTM		Db		db
1	4	500	20	8	8	.71	25	1	.37	562.48	2.57	22.19	1.45	2.5	18.64	30.1	21.57	31.45
2	4	500	25	10	10	.74	35	2	.85	580.8	1.50	68.09	1.60	5.0	37.06	36.15	40.47	36.91
3	4	500	30	12	12	.81	45	3	.91	591.1	4.26	44.59	2.39	6.5	54.44	30.49	60.09	40.35
4	4	750	20	8	10	.74	45	3	1.19	610.5	2.50	26.63	2.41	9.5	51.26	38.97	53.49	39.34
5	4	750	25	10	12	.81	25	1	1.27	576.5	3.17	60.26	1.68	7.0	49.35	38.64	54.59	39.51
6	4	750	30	12	8	.71	35	2	3.36	596.8	3.50	58.56	3.12	8.5	74.12	42.17	76.70	42.47
7	4	1000	20	10	8	.81	35	3	3.4	612.17	3.50	59.15	2.89	5.5	69.69	41.63	69.64	41.63
8	4	1000	25	12	10	.71	45	1	4.17	633.5	4.33	61.35	2.96	9.0	89.45	43.80	89.08	43.77
9	5	1000	30	8	12	.74	25	2	3.41	580.8	4.67	52.03	2.11	6.0	65.21	41.06	67.58	41.37
10	5	500	20	12	12	.74	35	1	2.18	587.1	1.50	43.26	2.15	10.5	51.54	39.01	53.70	39.37
11	5	500	25	8	8	.81	45	2	.82	649.3	1.66	22.61	2.32	4.5	40.12	36.84	36.97	36.13
12	5	500	30	10	10	.71	25	3	2.98	569.2	3.50	49.77	1.05	3.5	43.71	37.58	44.14	37.67
13	5	750	20	10	10	.71	45	2	1.04	580.9	3.66	43.73	2.62	5.0	48.02	38.40	53.11	39.27
14	5	750	25	12	12	.74	25	3	4.20	577.6	2.50	10.45	.33	5.0	33.63	35.31	27.96	33.70
15	5	750	30	8	8	.81	35	1	1.59	562.7	3.50	28.75	1.82	6.0	39.42	36.69	43.30	37.50
16	5	1000	20	12	12	.71	25	2	2.52	555	3.83	7.85	2.26	5.0	38.88	36.57	41.05	37.04
17	5	1000	25	8	8	.71	35	3	1.67	608.2	4.33	37.81	0.00	8.5	50.7	36.88	51.88	39.07
18	5	1000	30	10	10	.74	45	1	2.24	628.9	4.33	54.98	2.87	2.5	64.4	40.96	64.65	40.98
													TOTAL		919.7	692.32	949.4	697.5
													AVG		51.10	38.46	52.78	38.75

Table shows the mean squares of the various factors and their F-ratios. It can be seen that the inner gas, laser power, and overlap factor are very strong when compared to the experimental error, and the powder flow rate and federate are reasonably significant.

The confidence Interval (CD) is given by, $Cl_1 = \frac{\sqrt{F_{\alpha;lv2Vep}}}{N}$

Where $F_{\alpha;lv2V2}$ is the F-ratio required for α risk

$V_1 = 1$, V_2 = degree of freedom for the pooled error which is 6

V_{ep} = pooled error variance which is 3.3.6

n = number of tests in that condition which is 3

TABLE VI Percentage contribution

Factor	Mean Square	F-Ratio
Se^2	3.36	-
MS_p	23.35	6.95
MS_c	17.01	5.60
MS_{IG}	28.10	8.37
MS_{PF}	8.70	2.59
MS_F	7.41	2.121

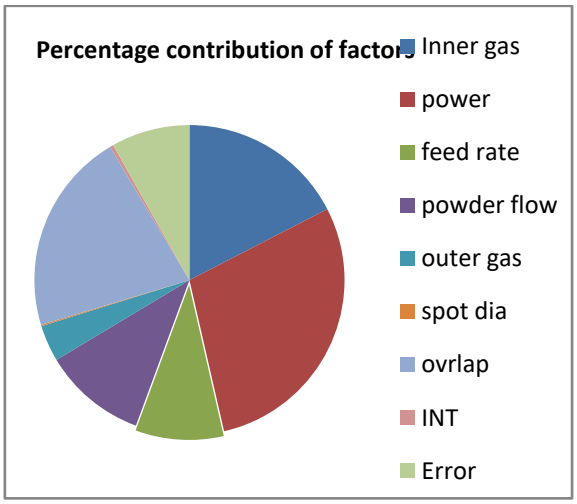

Fig. 2 Percentage contribution of factors

The optimized mean lies in a range given by $\pm CI_1$. The confidence interval estimate around the mean has a range of ±2.05 with 90% confidence, ±2.59 with 85% confidence, and , ±3.91 with 890% confidence. The confirmation experiment gave values of 77.19 from the mean and 42.52 for the S/N ratio showing that the experiment was successful and the additivity of the process is substantial enough for its control even in the presence of errors and interactions.

TABLE VII Mean Square and F-Ratios

SS for factors	Percent contribution	
SS(IG)	28.10	17.43
SS(P)	46.71	28.98
SS(F)	14.83	9.20
SS(PF)	17.40	10.79
SS(OG)	6.13	3.80
SS(D)	.23	.14
SS(O)	34.02	21.10
SS(INT)	.60	.37
SS(ERROR)	13.19	8.19

The predicated value for the mean 78.64 and the S/N ratio was 43.87. Another set of experiments was conducted for unequal distribution of weights from the OEC function and the result were listed in Table

II. CONCLUSION

The laser deposition process was thus optimized for build rate, micro-hardness, porosities SDAS, and ASTM grain size, and the optimal parameter combinations were found for the different weightage of OEC_s. The optimal values were predicted using the predictive mode and the confidence intervals were calculated. The confirmation experiments verified the model and fell within the confidence interval limits estimated. The system was made robust and controllable in the presence of interactions, noises and experimental errors, and the microstructure was also studied.

REFERENCES

[1]. El Cheikh, H.; Courant, B.; Hascoet, J.; Guillen, R., (2012) Prediction and analytical description of the single laser track geometry in direct laser fabrication from process parameters and energy balance reasoning, Journal of Materials Process Technology, 212, 1832–1839.

[2]. Gao, R.; Wang, L.; Teti, R.; Dornfeld, D.; Kumara, S.; Mori, M.; Helu, M. (2015) Cloud-enabled Prognosis for Manufacturing, CIRP Ann. Manufacturing Technology, 64, 749–772.

[3]. Riveiro, A.; Mejías, A.; Lusquiños, F.; del Val, J.; Comesaña, R.; Pardo, J.; Pou, J, (2014) Laser cladding of aluminium on AlSi 304 stainless steel with high-power diode lasers, Surface Coating Technology, 253, 214–220.

[4]. Ocylok, S.; Alexeev, E.; Mann, S.; Weisheit, A.; Wissenbach, K.; Kelbassa, I, (2014) Correlations of Melt Pool Geometry and Process Parameters during Laser Metal Deposition by Coaxial Process Monitoring, Physics Procedia, 56, 228–238.

[5]. Attar, H.; Ehtemam-Haghighi, S.; Kent, D.; Wu, X.; Dargusch, M.S, (2017) Comparative study of commercially pure titanium produced by laser engineered net shaping, selective laser melting and casting processes, Material Science Engineering, 705, 385–393.

[6]. Angelastro, A.; Campanelli, S.L.; Casalino, G, (2017) Statistical analysis and optimization of direct metal laser deposition of

227-F Colmonoy nickel alloy, Optical Laser Technology, 94, 138–145

[7]. Dutta, B., Palaniswamy, S., Choi, J., Song, L.J., Mazumder, J., (2011) Additive manufacturing by direct metal deposition, Advanced Materials & Processing, Vol.169 (5). Pp. 33–36

[8]. Leyens, C., Beyer, E., (2015) Innovations in laser cladding and direct laser metal deposition. Laser Surface Engineering, Pp. 181-192.

[9]. Li, S., Wei, Q., Shi, Y., Zhu, Z., Zhang,D.,(2015) Microstructure Characteristics of Inconel 625 Superalloy Manufactured by Selective Laser Melting, Journal of Materials Science & Technology, Vol.31, Iss. 9, Pp.946-952.

[10]. Wilson, J.M., Piya, C., Shin, Y.C., Zhao, F., Ramani, K.,(2014) Remanufacturing of turbine blades by laser direct deposition with its energy and environmental impact analysis, Journal of Cleaner Production, Vol. 80, 1 Pp. 170-178.

[11]. Fearon, E. and Watkins, K. (2004) Optimization of Layer Height Control in Direct Laser Deposition, 23rd International Congress on Applications of Laser & Electro-optics paper No. 1708.

[12]. Peng, L., Taiping, Y., Sheng, L., Dongsheng, L. Qianwu, H., Weihao, X., and Xiaoyan, Z. (2005) Direct Laser Fabrication of Nickel Alloy Samples Internaitonal Journal of Machine Tools and Manufacture" 45:1288-1294

[13]. Prakash .S (2004) Optimization of laser aided manufacturing process using the design of experiments approach-Taguchi way,Thesis", ,University of Missouri-Rolla 8431.